Wind Tunnels and Flight

by

Henry McDonald, James Ross, David Driver, and Stephen Smith

NASA Ames Research Center
Moffett Field, CA, 94035 USA

ABSTRACT

The problem of extrapolating wind-tunnel data to flight conditions has been with us since the early days of aviation. The Wright brothers faced the problem, as has everyone else who used wind-tunnel data as part of their aircraft design process. The techniques used for correcting wind-tunnel data for wall and mounting effects are applied meticulously, but they are usually limited to linear flow approximations. The remaining issues for extrapolation are geometric differences between models and airplanes, non-linear effects of wind-tunnel walls and mounting systems, and the effects of Reynolds number. These effects are poorly understood or difficult to predict and they can result in a new aircraft falling short of its guaranteed performance. The current practice in wind-tunnel data corrections are summarized and the missing physics identified. Current work on improving our understanding of the pertinent aerodynamics and to improve extrapolation methods are presented along with a discussion of further areas of inquiry.

1. INTRODUCTION

In view of the current limitations of predictive analyses, nearly all aircraft designs are tested in wind tunnels in order to accurately estimate performance. These wind tunnel tests are carefully performed to reduce the financial risk of missing the performance guarantees given to the buyers of the airplane. Mack and McMasters[1] reported in 1992 that a 1% reduction in drag was worth several million dollars per year to an operator's fleet of aircraft. Clearly, missing the drag or other performance guarantees on the negative side can result in significant economic penalties for a manufacturer. Even missing the performance on the positive side means that the design point was miscalculated, possibly resulting in an overly conservative design and reduced profit margin.

In order to minimize the possibility of such occurrences, aircraft manufacturers have developed rigorous testing procedures. The procedures are important not only to assure repeatable, high quality measurements but also to account for the fact that the aerodynamic characteristics of a model in a wind tunnel are not identical to that of the full-size airplane in flight. There are many aspects to this problem including wall and mounting interference, geometric fidelity of the model, and mismatches in Reynolds number. The schemes used for many of these corrections and for extrapolation to flight are tightly held by the aircraft industry because of the potential competitive advantage they may provide. In spite of the best engineering efforts in performing the extrapolations, there are still many instances in which some aspect of the aerodynamics or control of a new design fall short of requirements.

The reasons for these extrapolation errors are not fully understood, but are often attributed to the effects of Reynolds number. This is justified, to a large extent, because of the complex, Reynolds number sensitive fluid mechanics associated with the aerodynamic performance for both cruise and high-lift wing configurations. Figure 1 illustrates some of these complexities. Boundary-layer transition, shock/boundary-layer interaction, and flow separation near the trailing edge all affect cruise wing performance. For the multi-element airfoils associated with take-off and landing configurations, shock/boundary-layer interaction, attachment-line transition, confluent boundary layers, laminar separation bubbles, boundary-layer transition, and recirculating separated flows are the relevant complex flow features.

There has been considerable work aimed at reducing the uncertainty of Reynolds-number extrapolation. It is not easy, however, to completely separate the effects of aeroelastic model deformation from the true Reynolds number effects. In light of the importance and current uncertainties of the extrapolation process,

this research should continue and be augmented in both the theoretical and experimental areas. We will discuss some of this work in the context of how wind tunnels affect aircraft design. We will also present some current work with an emphasis on the experiments where laser techniques have provided important aero/fluid-dynamics measurements that were previously unavailable.

2. THE ROLE OF WIND-TUNNEL TESTING IN THE DESIGN PROCESS

The aerodynamic design processes used by aircraft manufacturers are varied and generally not fully disclosed to protect features of competitive advantage. For the purposes of this discussion however, a generic design process can be thought of as consisting of a conceptual phase, preliminary phase, and a final phase. During the conceptually design phase, simple analysis methods are used to determine the overall design features required to meet the proposed mission. The mission is a result of market surveys, customer requests, or projected new markets. The tools used to develop a conceptual design generally employ a large measure of empiricism and low-order aerodynamics computations. Using these tools, the designer can relatively quickly determine the span, wing area, overall length, propulsion requirements, and weight for an aircraft. It is in this phase of design where the likelihood of a commercially viable airplane, that might satisfy the given requirements, is first determined.

The next stage of the design process employs much more sophisticated analysis tools to determine the expected aerodynamic performance, weight, and cost of the airplane. A great deal of iteration between disciplines is required at this point in order to arrive at acceptable compromises and a design that can still carry out the desired mission. It is during this phase that wind tunnel testing may first begin. Much of the testing at this stage has been replaced by computational fluid dynamics (CFD) methods that now accurate enough to compute the cruise performance and to estimate the high-lift capability. Some wind tunnel testing may still be performed in order to assess a unique design feature or to validate the CFD generated information.

In the final design phase, cruise performance, control authority, off-design behavior, and high-lift performance must be accurately assessed. More of this work is done computationally as the methods are improved, but there remain sufficient shortfalls in both the accuracy of CFD as well as the ability to generate the quantity of data required to completely characterize the aerodynamic characteristics. Cruise performance is often predicted accurately by Reynolds Averaged Navier-Stokes (RANS) methods, but high-lift performance and off-design conditions are not. In addition, it is still much too time consuming to generate the large aerodynamic and stability and control databases using CFD.

2.1 Wind-Tunnel Data Correction

Given that the purpose of wind tunnel testing is to predict the performance and behavior of a vehicle in flight, it is important to make corrections or adjustments to wind tunnel data to account for differences between the wind tunnel and flight environments. These corrections generally fall into two categories. First, it is necessary to correct the data for the non-ideal flow environment of the wind tunnel created by the tunnel walls and the mounting system. Second, experimental procedures may be used to simulate higher Reynolds numbers than can be achieved in the wind tunnel.

Wind tunnels are normally designed with increasing cross-sectional area through the length of the test section to compensate for boundary layer growth on the walls. This compensation is never perfect, so a longitudinal pressure gradient exists in the test section that produces a buoyancy force on the model. Buoyancy corrections are made based on measurements of the empty-tunnel pressure gradient and the streamwise variation in model cross-sectional area. Stream angle corrections are made to account for errors in flow angle with respect to the wind-tunnel axis. To assess the stream angle correction, the model is tested upright and inverted. The reference stream angle is the angle that leads to matching lift curves for the two orientations.

The presence of any model in the wind tunnel also creates a local reduction of cross-sectional area, and an associated increase in local velocity. The effects of the locally elevated dynamic pressure caused by the constraining effect of the tunnel walls are normally determined by analytical or computational solutions of potential flow equations. This so-called blockage correction may in some cases be lumped together with

corrections for other wall-induced effects, such as the induced flow angles. The influence of the walls may be represented by the presence of a system of image vortex and source elements. These elements, in particular the image vortices, induce a net upwash on the model that leads to spurious reduction of induced drag on the model. Potential flow models may be used to determine the integrated upwash angle and induced drag increment associated with the image vortex system. Finally, the model support system may induce non-representative forces and moments on the model that must be corrected, normally by an incremental method using alternate or dummy supports. More detailed descriptions of basic wind-tunnel testing procedures and correction schemes can be found in the literature.[2-5]

In order to more closely match flight conditions, the state of the boundary layer on the model must be considered. In the case of fully turbulent, attached flow on both the model and the flight vehicle, a simple correction can be made for the reduction in skin friction coefficient with increased Reynolds number. The lower Reynolds number flow on the model however, is generally not fully turbulent. Therefore, the boundary layer on both the wing and fuselage is tripped using properly located and sized roughness elements. Unfortunately, a tripped, low-Reynolds number boundary layer does not behave the same as one experiencing natural transition at a higher Reynolds number. This is one of the driving factors in having very high Reynolds number test facilities. Various strategies exist for determining where to force boundary layer transition. The most obvious approach is to force boundary layer transition as close to the leading edge as practical to obtain a fully turbulent condition on the model. In this case, the drag data must be corrected for the change in skin friction coefficient with Reynolds number, and for the estimated drag of the transition device(s).

Another approach determines the transition location such that the momentum thickness at the trailing edge on the model matches that expected in flight. This would presumable give the correct drag level directly. For transonic transport aircraft, the shock position is strongly affected by boundary layer displacement thickness, and thinner laminar boundary layers may more accurately represent the displacement thickness at flight conditions. In this case, transition would likely be forced just ahead of the shock to avoid any unusual shock interaction with a laminar boundary layer. Corrections are then applied for the reduced skin friction in the laminar region as well as for the reduced turbulent drag and for the drag caused by trip devices.

An interesting fall out of the extrapolation issue is that companies tend to use specific wind tunnels for particular types of testing. This is because the engineers understand how the wall and mounting corrections are applied and they develop a base of experience with extrapolating measured performance to flight conditions for various airplanes tested in these particular wind tunnels. Moving to different wind tunnels requires recalibrating the engineers' understanding of the data obtained there and increases the uncertainty in using the data.

2.2 Other Extrapolation Issues

Once wind-tunnel data have been corrected to emulate flight conditions (at least to first order), additional corrections are still needed to obtain sufficiently accurate performance estimates. These include corrections for geometric fidelity (incomplete modeling of airplane details and different aeroelastic deformation of an airplane compared to its corresponding wind-tunnel model), and the non-linear effects of Reynolds number differences. Of these two general effects, geometry differences are responsible for the largest uncertainties in extrapolating wind tunnel data.

For cruise configurations, geometry corrections are made using both CFD and empirical methods. For excrescence drag in cruise, empirical methods are very effective. Industry engineers have a great deal of experience in accounting for the drag associated with airplane parts and details that are too small to reproduce accurately at model scale within a realistic budget. Aeroelastic deformation is accounted for by designing the model in the shape expected for 1-g flight. That means that the off-design conditions (particularly for higher g loadings) will not be measured for exactly the same configuration in the wind tunnel as occurs in flight. CFD can be used to estimate some of the aerodynamic effects of these deformations.

For flight conditions off of the cruise design point where incipient flow separation may exist, extrapolating to flight conditions is much more difficult because of non-linear Reynolds number effects. In particular, it is

3

difficult to extrapolate the margin in lift coefficient above cruise before the onset of buffet, and the change in pitch stability that occurs at that point. At some angle of attack above the cruise condition, some portion of the wing begins to experience significant transonic shock-induced separation. The characteristics of swept wings usually predispose the outboard wing sections to separate first, causing an inboard, and thus forward shift of the aerodynamic center. This forward shift is associated with an undesirable loss of pitch stability. Naturally it is paramount to know how severe this behavior is, and at what point it occurs.

The complex shock-boundary layer interactions involved in buffet onset are highly sensitive to Reynolds number. The sensitivity of shock location and strength to Reynolds number is shown in figure 2. These are computed pressure distributions from Goldhammer and Steinle[4] that show an increase in shock strength with increasing Reynolds number. The increase in adverse pressure gradient associated with Reynolds number could lead to earlier onset of buffet than expected if testing were performed at less than 50% of flight Reynolds number. The difficulty in extrapolating buffet onset to flight conditions is notionally illustrated in figure 3. The lift coefficient (C_L) for buffet onset as a function of Mach number is shown for two different airplanes. Included are curves for both the wind tunnel results and flight. Note that the extrapolation has a different sign for these two aircraft and the designers must know what causes this difference in behavior in order to avoid surprises.

CFD methods are emerging as a useful approach for determining and correcting for the influence of Reynolds number on buffet onset. Confident application of CFD to this problem requires extensive experimental validation and perhaps more importantly, detailed flow diagnostic measurement of turbulence and separation characteristics.

As uncertain as the picture is for buffet onset, it is even more uncertain for high-lift flight regimes. There are many more complex and interacting flow features for high-lift configurations than for cruise (figure 1). In addition, high-lift performance is very sensitive to the rigging of the flaps and slats relative to their neighboring elements. Because of this sensitivity, the brackets used to hold the slats and flaps on wind-tunnel models must be extremely stiff – often requiring that they be larger than would be given by physical scaling of the model. For example, the slat tracks on a particular transport aircraft are on the order of 4 cm wide. On a 4.2% model of the airplane that was tested in a pressurized low-speed wind tunnel, the large aerodynamic loading required slat brackets that would scale to nearly 8 cm wide on the airplane. The wider slat brackets shed larger wakes over the main element and flap which reduces the maximum lift of the model relative to more accurately sized brackets. Another concern for high-lift models is that the flap and slat elements themselves are not stiff enough to resist bending under load during testing, resulting in gap variations across their spans that are not representative of what is found on the actual airplane. These aeroelastic deformations of the model add uncertainty to the interpretation of the wind-tunnel data.

The high-lift performance of multi-element airfoils is also very sensitive to Reynolds number. A recent experiment examined the effect of Reynolds number on the aerodynamic performance of a 3-element high-lift system on a generic wing in the 12-Foot Pressure Wind Tunnel at NASA Ames Research Center. The results, for one particular rigging of the single-slotted flap and slat, are shown in figures 4 and 5. Figure 4 shows the lift curves at several Reynolds numbers, from 3.5 to 14.7 million. It is clear that Reynolds number (or dynamic pressure since it varies directly with Reynolds number in this wind tunnel) has an impact on the lift characteristics, changing the slope of the curve, the maximum lift, and the angle of attack at stall. The maximum lift coefficient (C_{Lmax}) is a parameter that directly affects the operating cost of an airplane since it limits the maximum weight. The variations shown in figure 5 are sufficient to cause an airplane to fail in meeting the manufacturer's guarantees. Given the variations shown for this range of Reynolds number (and dynamic pressure), it is unclear how to extrapolate to flight conditions (Reynolds number up to 50 million). This is particularly true since the relative importance of Reynolds number and deformation of the model cannot be easily determined.

New experimental techniques are now available to measure the deformation of models during testing. The measurements are done optically either by tracking the motion of markers on the model surface[6] or by Moire interferometry.[7] Simply knowing the deformation as a function of Reynolds number doesn't necessarily

clarify the extrapolation issues, but it will allow a more detailed examination of geometry versus flow physics using CFD.

To complicate the picture for high-lift, unsteady flows in the region of the slat and flap coves also have a strong influence on the aerodynamic performance and the detailed flow physics.[8-10] At this point there are insufficient data to determine whether the character of the unsteadiness changes with Reynolds number. What is clear is that the current state of the art in CFD does not capture this aspect of the flow over multi-element wings, limiting the use of computational methods in detailed high-lift design.

2.3 Aerodynamic Noise

Another area that is becoming more important in aircraft development is noise. With air traffic increasing at about 5% per year, many airports are limiting their hours of operation to reduce the noise impact on the surrounding community. As a result, manufacturers are looking seriously at noise as a market-limiting characteristic of new aircraft. While much of the noise is from the engine, the airframe (high-lift devices and landing gear) is a significant contributor, particularly during approach. Experiments in the 12-Foot Pressure Wind Tunnel have shown that there is a minimum Reynolds number below which airframe noise measurements may be as much as 2dB in error. Figure 6 shows the flap-tip noise sources on a transport aircraft at the same lift conditions for 2 different Reynolds numbers along with the associated spectra. This study showed that above a chord Reynolds number of approximately 3.5 million, the noise sources do not change. For this particular model, the lift curves also did not change above 3.5 million. This is a single result for a particular high-lift system and wing and may not be universally true. More work is needed to discern the complete connection between aerodynamics and airframe noise, in particular, the unsteady flows associated with multi-element airfoils.

Although rotorcraft issues are mostly outside the scope of this paper, noise is also a significant issue for helicopter and tiltrotor operations. Blade vortex interaction (BVI) noise that occurs during descending flight can be very loud and may limit rotorcraft operations at some airports because of community annoyance. The location and strength of the rotor wake relative to the rotor blades are important for BVI noise generation, so proper modeling of BVI intensity and directionality and the evaluation of potential noise reduction schemes require that the dynamics and aerodynamics of the rotor are adequately represented. Hence, measurements of BVI noise are ideally performed on large or full-scale models, which require large testing facilities in order to measure noise in the far-field (typically 1-2 rotor diameters). These far field measurements can then be used to extrapolate to flight/fly-over conditions.[12] Dynamically scaled small-scale rotors are also used for BVI investigations. The benefit of using small-scale rotors in a large wind tunnel is that far field noise directionality can be mapped over a greater area than for a full-scale rotor. In either case, large wind tunnel facilities with low background noise and anechoic walls are critical for rotorcraft BVI measurements.

2.4 Wind-Tunnel Flow Quality

The observation that different wind tunnels give different answers for the same model and nominal flow conditions has been recognized since the early 1900's. Bacon and Reid[13] summarized the difference in critical Reynolds number for spheres in different wind tunnels. They attributed the differences to the variations in both mounting system and free-stream turbulence. Several years earlier, Prandtl[14] suggested that the drag of a sphere be used to characterize the turbulence levels of wind tunnels. For many years, the transition Reynolds number of a sphere was used as a measure of flow quality in wind tunnels.

As engineers improved the flow quality in wind tunnels, the correlation with sphere drag was insufficient to discern subtle turbulence effects. Research at DFVLR in the 1980s indicated that aside from turbulence intensity, the frequency content of the free stream plays a role in causing premature transition.[15] That work looked at boundary-layer transition on a 6:1 prolate spheroid in several low-speed wind tunnels. For higher speeds, a $10°$ cone has been used in a similar manner to characterize the influence of free-stream turbulence on boundary-layer transition. Dougherty and Fisher[16,17] provided the most extensive database on the subject looking at both wind-tunnel and flight data for the same cone model. Wolf and Laub[19] also used a $10°$ cone in a later study to characterize the flow in a new quiet supersonic wind tunnel.

More recently, Watmuff[19] showed that transition on a flat plate is extremely sensitive to free-stream disturbances. In his meticulously run experiment, he found that a flow with nearly immeasurably small non-uniformities in the free-stream still has a large effect on the growth of instability waves in the boundary layer. In this experiment it was not the free-stream turbulence (~0.05% in the axial direction) but the small velocity defects remaining from screen non-uniformities that affected boundary-layer stability.

This sort of research will help us to understand the effect that free-stream turbulence has on aerodynamics measurements, but will require a long-term commitment in order to connect the fundamental fluid mechanics to measured aerodynamic performance. Of particular importance are the conditions leading to rapid changes caused by nonlinear viscous effects (e.g. onset of flow separation).

2.5 Arcjet Flow State

For hypersonic flight, one of the most important features to model is the heat transferred to the vehicle. The arcjet is the best way to simulate that harsh flow environment. Fundamentally, arcjets provide a long duration (10's of minutes) of high enthalpy flow that simulates the local heating environments expected for high-speed trans-atmospheric vehicles such as reusable launch vehicles (RLV) and planetary entry probes. The process of generating high enthalpy flows result in a highly energized, supersonic free stream that is very complex in that it is not in chemical equilibrium and contains gas species in excited states in a frozen flow regime. This is not an exact analog for the flight conditions in which the vehicle experiences a strong bow shock generated in a relatively cold and quiescent atmosphere that is in thermal and chemical equilibrium.

The development of the next generation of reusable launch vehicles will demand significant improvements in NASA's Thermal Protection System (TPS) technology to achieve the required safety and reliability. TPS development requires understanding of testing conditions in arcjet flows such as enthalpy, pressure, temperature, velocity, species states, and their distribution within the arcjet flow free stream. Arcjets have been primarily used to test heating environments 'local' to TPS test articles. There has been a strong emphasis on improving the understanding of the response of TPS materials, especially in areas of energy accommodation due to surface catalytic recombination, through measurements and modeling analysis. Furthermore, since the arcjets only simulate flight conditions, rather than duplicate them, obtaining 'traceablility to flight' has been an issue. There is a need to improve the characterization of arcjet flow fields and corresponding CFD modeling.

The challenges of TPS development are even more difficult for ablating TPS materials, since the material actively participates (and alters) the local flow field around the TPS. In addition to critical needs in improved arcjet characterization[20] and modeling for TPS development, future capabilities are sought which will enable arcjets to be used as aerothermodynamic test facilities for use in sub-scale testing of TPS components and vehicles.

3. CURRENT RESEARCH ACTIVITIES

A great deal of work has been done on improving the understanding of various aspects of aerodynamics pertinent to design and testing. More recently, the experimental research has concentrated on validation of computational methods. These efforts have ranged from idealized model problems to full aircraft geometry. A sampling of these experiments are summarized below. Much of the work cited here was performed at NASA Ames Research Center, but this is not to imply that work in this area is not done elsewhere, just that these results were more readily available to us.

3.1 Transonic Buffet Experiment

The discussion above described some of the problems in predicting the onset of buffet either computationally or experimentally. One study of this subject is that described by Olsen, et al[21], which included both computations and experiments to document the current ability of CFD to predict the onset of buffet on a realistic transonic wing. A photo of the model is shown in figure 7. The tests were performed in the High Reynolds Number Channel #2 at NASA Ames Research Center.[22] This is a small pressurized wind tunnel that can run at up to 7 atmospheres and Mach numbers up to 0.9. The maximum Reynolds number for the experiment was 12 million, i.e. 25-50% of flight values.

Figure 8 shows the pressure distributions for a condition of shock-induced separated flow. The computed pressures in this case do not match the experiment very well. The computations miss the shock location but the authors report that the separation point is closely predicted (and that the computations predict attached flow cases quite well). This indicates that the shape of the separated wake is incorrect, affecting the shock location and the resulting loads on the wing. The computations also do not show the same sensitivity to Reynolds number as the measurements indicate. The computations clearly are missing some aspect of the flow physics, more than likely it is in the turbulence modeling in the RANS code. Further work is required in this area including well-coordinated experiments and computations as well as flight experiments, which are necessary in order to understand buffet onset in the flight environment.

3.2 Wake in Adverse Pressure Gradient

Accuracy of CFD predictions for separated flow fields is a strong function of the accuracy of the turbulence model used in such flows. While there has been much improvement in turbulence modeling of separated flows in the past 15 years (e.g. the use in design codes of models such as Johnson-King, SST(k-ω), and Spalart-Allmaras and other more realistic models) there remains a tendency to under-predict the size of the separation. Improvements to turbulence modeling are still required and demand high fidelity experiments. Accurate measurements of the turbulent fluctuation correlations (in particular the Reynolds shear stresses) are essential. These data are then used to guide the turbulence modeling effort.

One example of an experiment used to guide turbulence modeling for high-lift aerodynamics is a study of a wake in an adverse pressure gradient performed by Driver and Mateer[23] in the NASA Ames High Reynolds Number Channel #1. Flow behind a splitter plate was made to reverse direction by virtue of the adverse pressure gradient induced on the flow by a divergent wall test section (figure 9). This flow is an analog of wake of the main element encountering an adverse pressure gradient as it passes over a highly deflected flap on a wing configured for landing. Data were obtained with a 2 component LDV system with a 100 micron interrogation volume operating in back scatter and using Fourier transform signal processing. Flow reversal can be seen in the wake downstream of the splitter plate (figure 9). Superimposed on the streamlines shown in figure 9 are the measurements of the –uv Reynolds shear stress. A rapid growth in the shear stress is seen with distance along the separation – CFD usually predicts an even faster growth in Reynolds shear stress. These data are currently being used to examine the ability of a number of turbulence models to accurately reproduce this flow field.

3.3 PLANAR-DOPPLER VELOCIMETRY EXPERIMENTS

A relatively recently developed optical technique, called Planar Doppler Velocimetry (PDV), is capable of determining instantaneous, three-dimensional velocity vectors of moving particles or solid material in a laser light sheet everywhere in the field of view.[24-27] The measurements depend on directly detecting the Doppler shift in the laser light caused by the relative motion between the reflecting material in the flow and the camera. PDV holds the promise of being very well suited for use in large wind tunnels in which large areas of the flow field are of interest.

3.3.1 Flap-Tip Vortex

One of the early large wind tunnel applications of the technique was during a study of airframe noise in the 7-by 10-Foot Wind Tunnel at NASA Ames Research Center.[28] The model mounted in the wind tunnel is shown in figure 10. It is a modified 2-D, multi-element airfoil arrangement with the flap extending across half the span. In the photograph, the slat extends across the 75% of the span but it could also extend across the full span or removed completely.

Figure 11 shows the 3-component wake measurements ~1 m downstream of the flap tip/trailing edge. In this case, the leading edge slat was not present. From left to right, the figure shows the streamwise, spanwise, and normal velocities. The streamwise velocity contours clearly show the viscous wake from the wing and flap rolling up into the tip vortex. The other two components show the characteristic signature of a vortex.[28]

3.3.2 Rotor wake in Forward Flight

A recently completed experiment in the 80- by 120-Foot Wind Tunnel at NASA Ames Research Center examined the wake from a full-scale rotor in forward flight at one azimuthal station.[27] Three measurement cameras observing the plane of interest from 3 different angles provided the information necessary to determine all three components of velocity. The set up for the experiment is shown in figure 12. One instantaneous measurement is shown in figure 13. The color contours indicate the velocity normal to the measurement plane while the vectors show all 3 components. This proof-of-concept test demonstrated the viability of PDV measurements in the large wind tunnel but further development is needed to generate uniform seeding (particularly in the open return 80- by 120-Foot Wind Tunnel) and to obtain the ~1 m/s accuracy demonstrated in laboratory experiments.

3.4 PARTICLE IMAGE VELOCIMETRY EXPERIMENTS

Particle Image Velocimetry (PIV) is another method of acquiring instantaneous measurements of fluid velocities in a plane. Small tracer particles are introduced to the flow and short pulse duration, high-powered laser light sheets illuminate and freeze the motion of the particles. The positions of the tracer particles are captured using a standard photographic lens in conjunction with a digital camera. The displacement of the tracer particles over a short duration of time is used to calculate fluid velocities from two sequential digital images. A number of researchers have refined this technique to the point of being practical for use in large wind tunnels.[29-31]

3.4.1 High-Lift Aerodynamics

One of the aspects of high-lift aerodynamics and noise generation that is least understood is the flow around the lee-side of the leading-edge slat. As shown in figure 1, there is a relatively large area of separated flow with a reattachment point very close to the slot between the slat trailing edge and the main element leading edge. This is an area of very large velocity fluctuations and it is also a relatively large noise source. It is also responsible for generating a very unsteady wake downstream of the slat. Hot-wire measurements are difficult to obtain in this area (but have been obtained[8,9]) because of the large variation in mean-flow direction and the problems associated with traversing a probe through the region. Optical access for LDV measurements is also very limited. PIV offers a very attractive (though still challenging) method for obtaining a comprehensive set of data throughout the region of interest.

Figures 14a and b show PIV measurements behind the slat for a Mach number of 0.1, a 25° slat deflection (nose down), and 10° angle of attack.[9,31] The model used in this investigation is the same as is shown in figure 10. Only two velocity components were obtained in this experiment, primarily because of the difficult optical access but also because the spanwise velocity component is small in this region and it is probably not an important component of the unsteady flow. The mean velocities, obtained from an average of 100 instantaneous measurements, are shown in figure 14a. The region of recirculating flow is very apparent, as is the large acceleration of the flow approaching the slat gap. Figure 14b shows a measure of the flow unsteadiness, $TKE = (u'^2 + v'^2)/U_8^2$, which gives an indication of where the unsteadiness originates and how it might affect both the mixing of the slat wake over the main element and the noise generated in the slot. Figure 14c shows the contours of the same unsteadiness parameter for a lower slat deflection (5°). The lower slat deflection increases the aerodynamic load on the slat and the unsteadiness is very much reduced.

A similar experiment was performed in the Basic Aerodynamics Research Tunnel at NASA Langley Research Center.[10] The focus of that experiment was on the wake of the slat as it passes over the main element. The wake was measured using a 2-D PIV system. A different 3-element, 2-D airfoil was used in this experiment although the shape of the slat was the same as in the previously described study. The same conclusions were reached concerning the reduction in the wake unsteadiness with increased aerodynamic loading on the slat (angle of attack in this case). Much more work remains in this area if we are to develop a full understanding of the effects of the unsteady shear layers, both in the wake and on the lee-side of a slat,s and to relate these flow features to noise production.

3.4.2 Rotor Wake in Hover

The measurement of rotor wake velocities has been performed using a number of techniques, both point-wise and planar (see PDV measurements above). PIV is another method by which an entire plane of data can be obtained simultaneously. 3D PIV is particularly attractive for this application.

Measurements of a two-bladed rotor on a hover test stand were made using 3D PIV at the Army Hover Chamber at NASA Ames Research Center (figure 15)[32]. Equipped with rectangular-planform NACA 0012 blades, the rotor had a diameter of 2.3 meters and a chord of 19.1 cm. With the collective set at –8° and a rotor rpm of 870, the tip Mach number was 0.31 and the thrust coefficient was 0.005.

Figure 16 shows one set of instantaneous data of the rotor wake where the first blade is 30° past the laser plane and the second blade is at 210°. Figure 16a shows the in-plane velocity vectors and color contours indicating the out-of-plane velocity. Figure 16b shows the same data with vorticity shown in the contours. The vortex generated by the blade at 30° is located in the lower left of the plots. The wake from the other blade is above and to the right of the earlier vortex. The vortex from the second blade shows some distortion due to the presence of the viscous wake defect. The vorticity plot shows that the strength of the shed vortices remains relatively constant. Similar experiments have been performed at the Duits-Nederlandse 8- by 6-Meter Wind Tunnel for rotors both in hover and in forward flight.[33]

Having the ability to resolve an instantaneous plane of velocity data offers the opportunity to perform meaningful time-averaging of unsteady vortex fields. In particular, it is possible to eliminate the smearing effect that vortex wander has on pointwise measurements. The problem is that a pointwise measurement is at a fixed point in space. If the measurement is near the core of a vortex and the vortex moves randomly relative to its mean position, the resulting point measurement becomes both a time and spatially averaged quantity (relative to the vortex center). This problem is particularly acute for vortices since the velocity gradients are large near the core. Using PIV, the center of the vortex can be determined in every instantaneous velocity measurement and both the vortex motion and the instantaneous velocity distribution can be determined. The coordinate system can then be tied to the center of the vortex and a meaningful time average of the vortex structure can be determined.

Tiltrotor aircraft are relatively new in the operational air fleet of the US Marines (V-22) and will soon be part of the civil aviation fleet (Bell 609). The recent crash of a V-22 may have been caused by the so-called vortex ring mode in which the descent rate is approximately equal to the rotor downwash velocity causing a significant loss of lift. This is suspected to be a problem only when the forward speed is very low because vortex ring mode has been observed only at low forward speed on helicopters. The differences in the disk loadings of helicopters and tiltrotors and the substantially larger twist on tiltrotor blades require that further experiments be done to better understand the phenomenon. Another area of interest for tiltrotors and helicopters is in operating in the wakes of buildings, oil rigs, and ships. Wind-tunnel experiments, both large and small scale, are currently underway and will play an important role in understanding these problems and possible design or operational changes to eliminate them. Non-intrusive, laser-based measurements will play a large role in these experiments.

3.4.3 Wake Vortices

One of the hard limits on airport traffic growth is the restriction placed on the spacing of aircraft in the terminal area. The minimum spacing is set to assure that catastrophic encounters with wake vortices do not happen at altitudes too low to allow safe recovery. There has been a great deal of work in assessing the safety hazard posed by wake vortices[34,35] but so far, no practical ways to reduce the rotational velocities in the wake have been identified. A number of researchers have recently looked at the physics of aircraft wake roll up with the intent of finding ways to reduce the hazard. Dieterle, et al[36] used PIV to measure the wake generated by a transport aircraft model in free flight after having been launched from a catapult. Chen, et al[37], and Bristol, et al[38] examined the details of the wake roll up process behind a rectangular wing with a simulated flap segment. These measurements were made using a 2-D PIV system in a water tow tank. In this arrangement, the measurement plane remained fixed and the model towed through it and down the channel. The time history of the roll up was recorded from which the 3-D evolution of the wake in the measurement

plane was reconstructed. These measurements show details not easily seen in air which may lead to a better understanding of the physics and possible alleviation techniques. Figure 17 shows one such measurement as an iso-surface of vorticity. There is a great deal of interaction between the 4 vortices shed by the wing, which is very important to the wake-vortex hazard problem and the possibility of alleviation.

4. CONCLUDING REMARKS

In spite of tremendous progress in both CFD and wind tunnel capability, there is still significant risk in extrapolating wind-tunnel results to flight conditions. This places aircraft manufacturers at risk whenever they introduce new products. The remaining open issues are in the geometric fidelity of wind tunnel and computational models relative to flight vehicles, Reynolds number extrapolation, and effects of wind-tunnel flow quality. Because of the uncertainty in extrapolation, further research is needed in order to understand the sources of the uncertainty and ways to overcome them. More experimental research is also needed to improve the predictive capability of CFD methods so that they may be used with confidence in a wider range of flight/design conditions. This work will require advanced, non-intrusive measurement techniques in order to generate the high quality data to gauge computational results against.

References

1. Mack, M.D. and McMasters, J.H., "High Reynolds Number Testing in Support of Transport Airplane Development," AIAA paper 92-3982, 17th AIAA Aerospace Ground Testing Conference, Nashville, TN, July 6-8, 1992.

2. Rae, W. H., Jr. and Pope, A., *Low-Speed Wind Tunnel Testing,* John Wiley & Sons, New York, 1984.

3. Herriot, J.G.: Blockage Corrections for Three-Dimensional-Flow Closed-Throat Wind Tunnels, with Consideration of the Effect of Compressibility. NACA Report 995, 1950.

4. Goldhammer, M.I. and Steinle, F.W., "Design and Validation of Advanced Transonic Wings Using CFD and Very High Reynolds Number Wind Tunnel Testing," 17th ICAS Congress, Stockholm, Sweden, Sept. 9-14, 1990, Proceedings Vol. 1, AIAA, Inc., Washington DC, 1990, pp. 1028-1042.

5. Ewald, B. F. R. (editor), "Wind Tunnel Wall Correction," AGARDograph 336, North Atlantic Treaty Organization, October 1998.

6. Burner, A. W. and Martinson, S. D., "Automated Wing Twist and Bending Measurements Under Aerodynamic Load," AIAA paper 96-2253, 19th AIAA Advanced Measurement and Ground Testing Technology Conference, New Orleans, LA, June 1996.

7. Flemming, G. A., Soto, H. L., South, B. W., and Bartram, S. M., "Advances in Projection Moire Interferometry Development for Large Wind Tunnel Applications," SAE paper 1999-01-5598, 1999 SAE/AIAA World Aviation Congress, San Francisco, CA, October, 1999.

8. McGilnley, C. B., Anders, J. B., and Spaid, F. W., "Measurements of Reynolds Stress Profiles on a High-Lift Airfoil," AIAA paper 98-2620, 16th AIAA Applied Aerodynamics Conference, Albuquerque, NM, June 1998.

9. Moriarty, P. J., Unsteady Measurements of a Three-Dimensional High-Lift System, PhD Dissertation, Stanford University, May 2000.

10. Paschal, K., Jenkins, L., and Yao, C., "Unsteady Slat-Wake Characteristics of a High-Lift Configuration," AIAA paper A00-16070, 38th AIAA Aerospace Sciences Meeting & Exhibit, Reno, NV, January 10-13, 2000.

11. Hayes, J., Horne, W., Jaeger, S., and Soderman, P., "Measurements of Reynolds Number Effect on Airframe Noise in the 12-Foot Pressure Wind Tunnel," AIAA paper 99-1959, 5th AIAA/CEAS Aeroacoustics Conference, Seattle, WA, May 10-12, 1999.

12. Signor, D. B., Watts, M. E., Hernandez, F. J., and Felker, F. F., "Blade-Vortex Interaction Noise: A Comparison of In-Flight, Full-Scale and Small-Scale Measurements,"

13. Bacon, D.L. and Reid, E.G., "The Resistance of Spheres in Wind Tunnels and in Air," NACA Report No. 185, *Ninth Annual Report of the National Advisory Committee for Aeronautics - 1923*, Government Printing Office, Washington DC, 1924.

14. Prandtl, L., "Der Luftwiderstand von Kugeln," Nachr. D. K. Ges. D. Wissensch, Gottingen, Math. phys. Kl., 1914, p. 177.

15. Meier, J. U., Michel, U., and Kreplin, H.-P., "The Influence of Wind Tunnel Turbulence on the Boundary Layer Transition," *Perspectives in Turbulence Studies*, Springer– Verlag, Heidelberg, Germany, 1987.

16. Dougherty, N.S. and Fisher, D. F., "Boundary Layer Transition on a 10-Degree Cone: Wind Tunnel/Flight Data Correlation," AIAA Paper 80-0154, 18th AIAA Aerospace Sciences Meeting, Pasadena, CA, January 1980.

17. Fisher, D. F. and Dougherty, N. S., "In-Flight Transition Measurement on a 10° Cone at Mach Numbers from 0.5 to 2.0," NASA TP-1971, June 1982.

18. Wolf, S. W. D. and Laub, J. A., "NASA Ames Laminar Flow Supersonic Wind Tunnel (LFSWT) Tests of a 10° Cone at Mach 1.6," NASA TM-110438, March 1997.

19. Watmuff, J.H., "Detrimental Effects of Almost Immeasurably Small Freestream Nonuniformities Generated by Wind-Tunnel Screens," AIAA Journal, Vol. 36, No. 3, pp 379-386, March 1998.

20. Fletcher, D. G. and Bamford, D. J., "Arcjet Flow Characterization Using Laser-Induced Fluorescence of Atomic Species," AIAA Paper No. 98-2458, 7th AIAA/ASME Joint Thermophysics and Heat Transfer Conference, 1998.

21. Olsen, M.E., Driver, D.M., Shairer, E.T., and Naughton, J., "The ROCK (AST-1) Wing: Design, Experiment, and Computation," AIAA Paper 2000-0670, AIAA 38th Aerospace Sciences Meeting and Exhibit, Reno, NV, January 10-13, 2000.

22. McDevitt, J. B., Poleck, T. E., and Hand, L. A., "A New Facility and Technique for Two-Dimensional Aerodynamic Testing," Journal of Aircraft, Vol. 20, No. 6, 1983, pp. 543-551.

23. Driver, D. M. and Mateer, G. M., "Wake Flow in an Adverse Pressure Gradient," to be presented at the SAE/AIAA World Aviation Congress, San Diego, CA, Oct. 10-12, 2000

24. Meyers, J. F., "Doppler Global Velocimetry. The Next Generation?," AIAA 91-0337, 29th AIAA Aerospace Ground Testing Conference, Nashville, TN, January 6-8, 1992.

25. Elliott, G. S. and Beutner, T., J., "Molecular Filter Based Planar Doppler Velocimetry," Progress in Aerospace Sciences, Pergamon Press, Vol. 35, 1999, pp. 799-845.

26. Reinath, M. S., "Doppler Global Velocimeter Development for Large Wind Tunnels," accepted for publication in Institute of Physics *Journal of Measurement Science and Technology*.

27. McKenzie, R.L. and Reinath, M.S., "Planar Doppler Velocimetry Capabilities at Low Speeds and Its Application to a Full-Scale Rotor Flow," AIAA Paper No. 2000-2292, 21st AIAA Advanced Measurement Technology and Ground Testing Conference, Denver, CO, June 19-22, 2000.

28. Storms, B. L., Hayes, J. A., Ross, J. C., and Moriarty, P. J., "Aeroacoustic Measurements of Slat Noise on a Three-Dimensional High-Lift System," AIAA Paper 99-1957, 5th AIAA/CEAS Aeroacoustics Conference, Seattle, WA, May 1999.

29. Adrian, R. J., "Particle-Imaging Techniques for Experimental Fluid Mechanics," Annual Review of Fluid Mechanics, Vol. 23, pp. 261-304, 1991.

30. Hoffman, J. M., Arnette, S. A., Porter, C. B., Sung, B., and Arik, B. E., "Application of Particle Image Velocimetry in the Korea Aerospace Research Institute Low Speed Wind Tunnel," AIAA Paper A 00-16309, 38th AIAA Aerospace Sciences Meeting & Exhibit, Reno, NV, January 10-13, 2000.

31. Moriarty, P. J. and Heineck, J. T., "PIV Measurements Near a Leading-Edge Slat," Proceedings of the Third International Workshop on PIV, Santa Barbara, CA, Sept. 16-18, 1999.

32. Heineck, J., Yamauchi, G., Wadcock, A., and Lourenco, L., and Abrego. A., "Application of Three-Component PIV to a Hovering Rotor Wake," AHS Forum 56, Virginia Beach, VA, May 2000.

33. Yamauchi, G. K., Burley, C. L., Mercker, E., Pengel, K., and JanakiRam, R., "Flow Measurements of an Isolated Model Tilt Rotor," AHS paper presented at AHS 55th Annual Forum, Montreal, Canada, May 25-27, 1999.

34. Rossow, V. J., "Lift-Generated Voprtex Wakes of Subsonic Transport Aircraft," Progress in Aerospace Sciences, Vol. 35, No. 6, pp. 507-660, Aug. 1999.

35. Spalart, P. R., "Airplane Trailing Vortices," Annual review of Fluid Mechanics, Vol. 30, pp. 107-138, 1998.s

36. Dieterle, L, Ehrenfried, K., Stuff, R., Scheider, G., Coton, P, Monnier, J. C., and Lozier, J. F, Quantitative Flow Field Measurements in a Catapult Facility Using Particle Image Velocimetry," Proc. Of the 18th International Congress of Instrumentation in Aerospace Simulation Facilities (ICIASF), Toulouse, France, pp. 1.1-1.10, June 21-24, 1999.

37. Chen, A. L., Jacob, J. D., and Savas, Ö., "Dynamics of Corotating Vortex Pairs in the Wakes of Flapped Airfoils," Journal of Fluid Mechanics, Vol. 382, 155-193, 1999.

38. Bristol, R., Ortega, J., and Savas, Ö., " A towing tank study of airfoil wake vortices at Re of order 10^5," AIAA Paper 99-3419, 1999
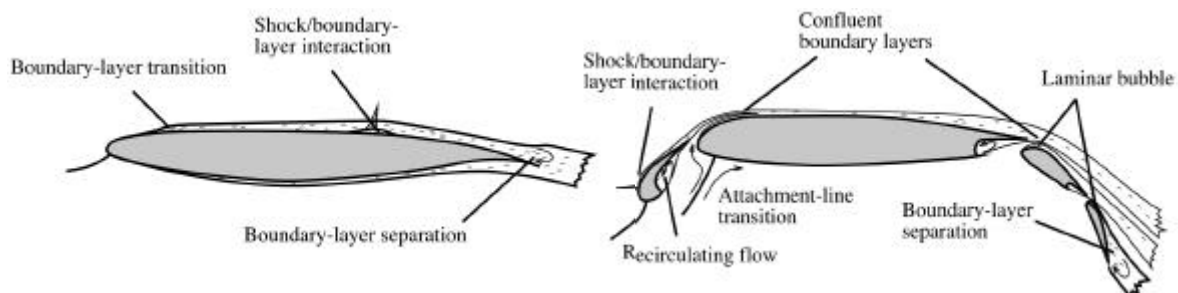
Figure 1. Flow physics associated with Reynolds number sensitive aerodynamics.[1]

3D RANS solutions
Pressures at 75% span
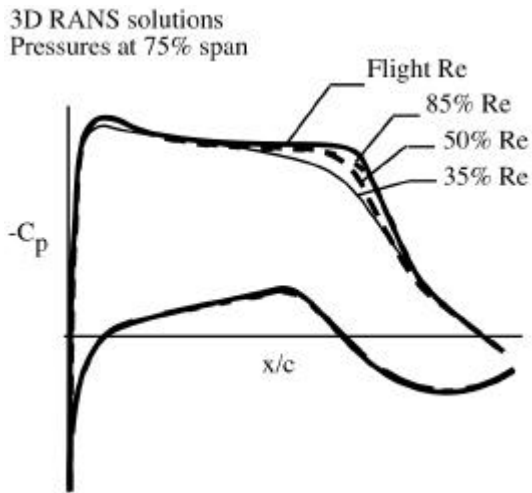
Figure 2. Computed effect of Reynolds number
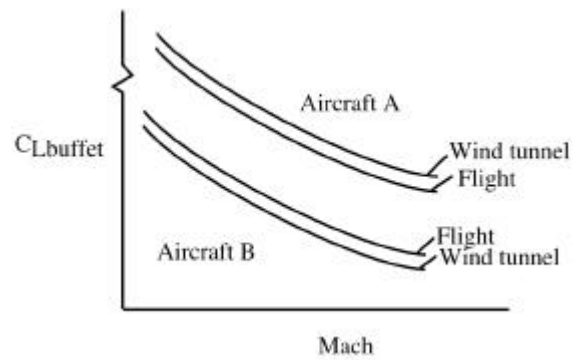on transonic wing pressure distribution.[4]

Figure 3. Inconsistency in extrapolating buffet
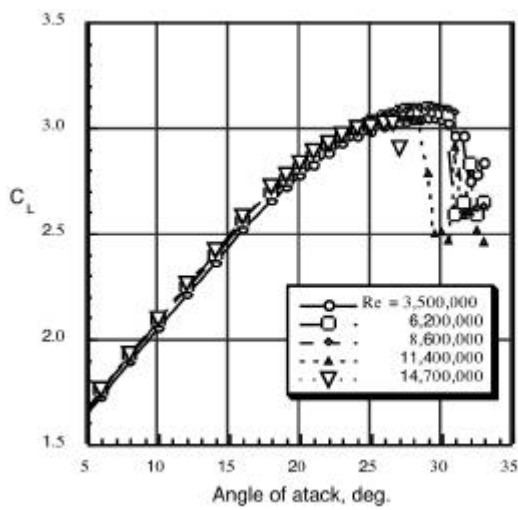onset from wind-tunnel data to flight
conditions.

Figure 4. Effect of Reynolds number on the lift of
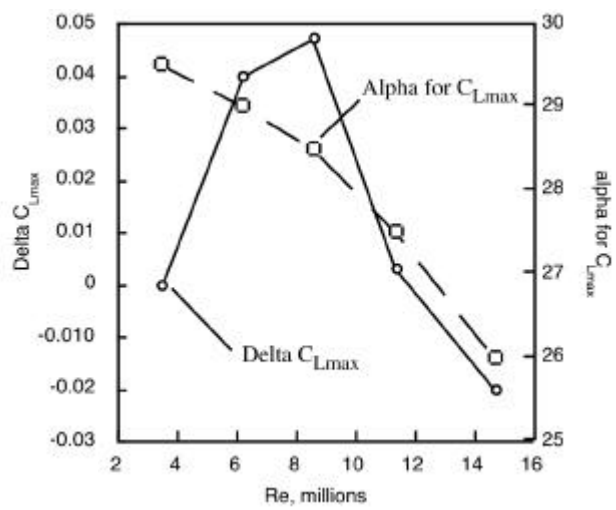a generic 3-element high-lift wing, $M =$
0.15.

Figure 5. Effect of Reynolds number on C_{Lmax}
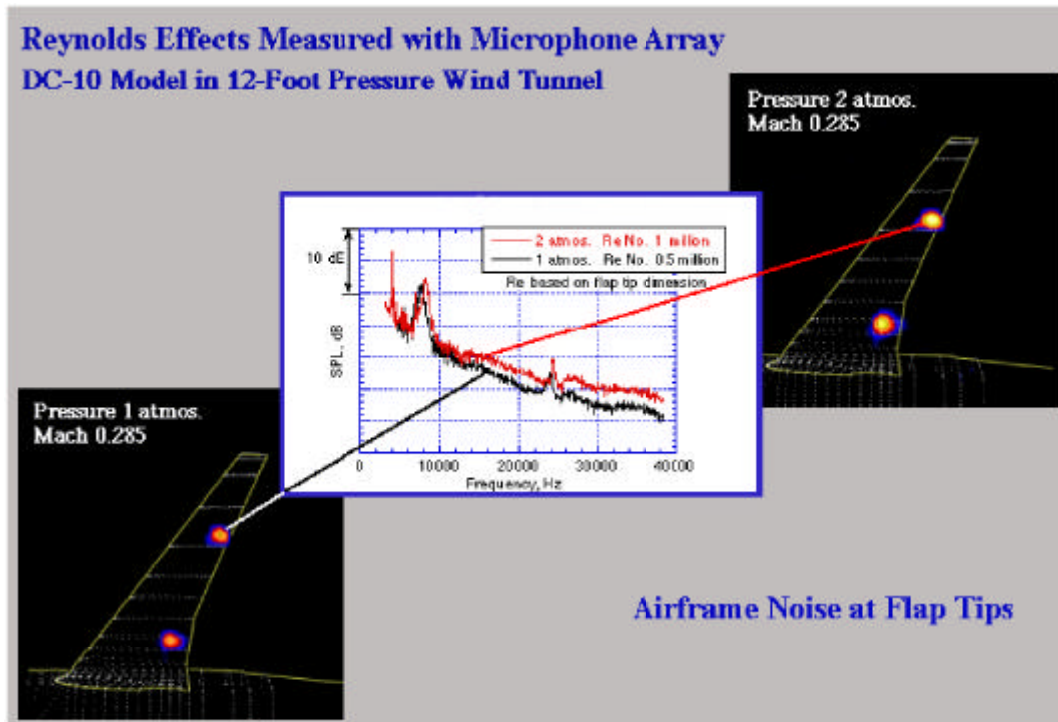and angle of attack for C_{Lmax} for same
generic wing.

13

Figure 6. Effect of Reynolds number on airframe noise. Color contours are sound pressure levels at 15 kHz measured using a phased microphone array. The spectrum was obtained by integrating the source levels at each frequency.[11]
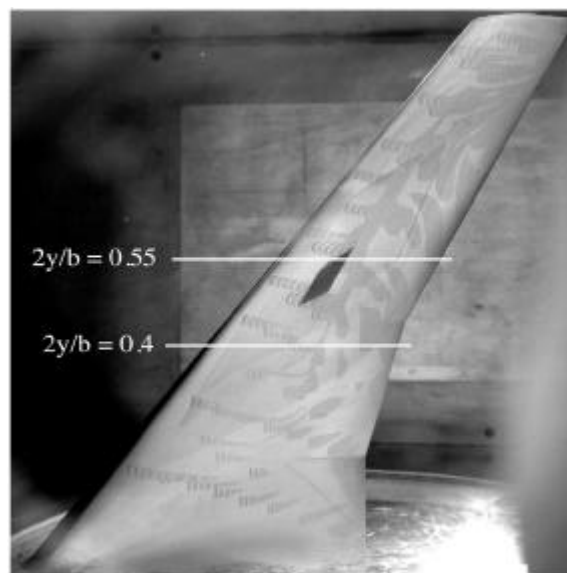
Figure 7. Photograph of the generic transonic wing in High-Reynolds number Channel #2. Darker patches are from oil film; the spacing of dark and light areas of oil indicate the level of skin friction. Spanwise locations noted are where data was taken in following figure.

14
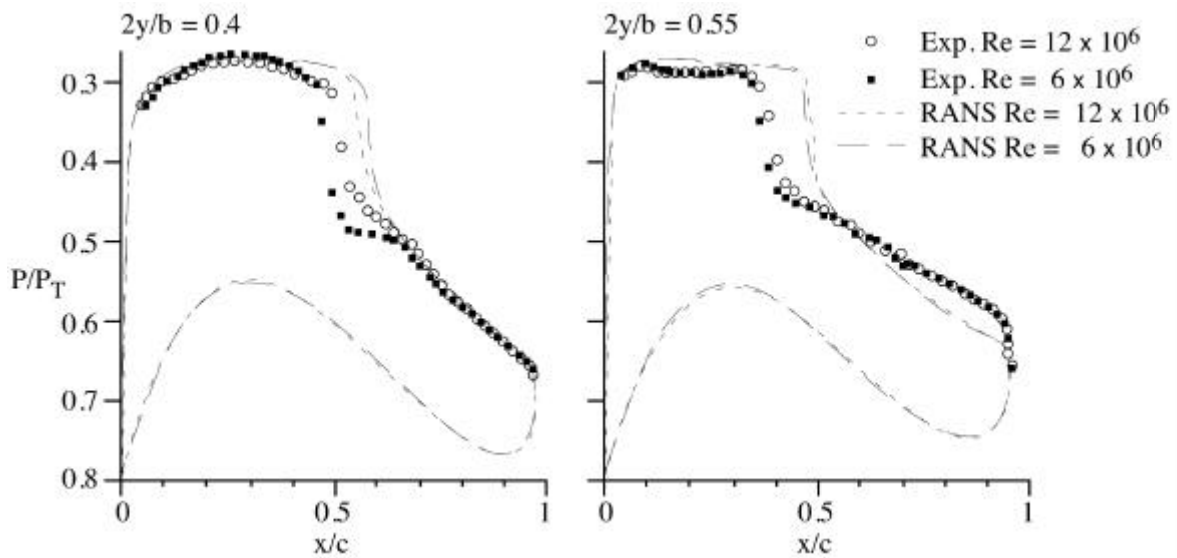
Figure 8. Measured and computed pressure distributions for generic transonic wing in figure 7 showing Reynolds number sensitivity at two spanwise locations; M = 0.8 and 2.75° angle of attack.[21]
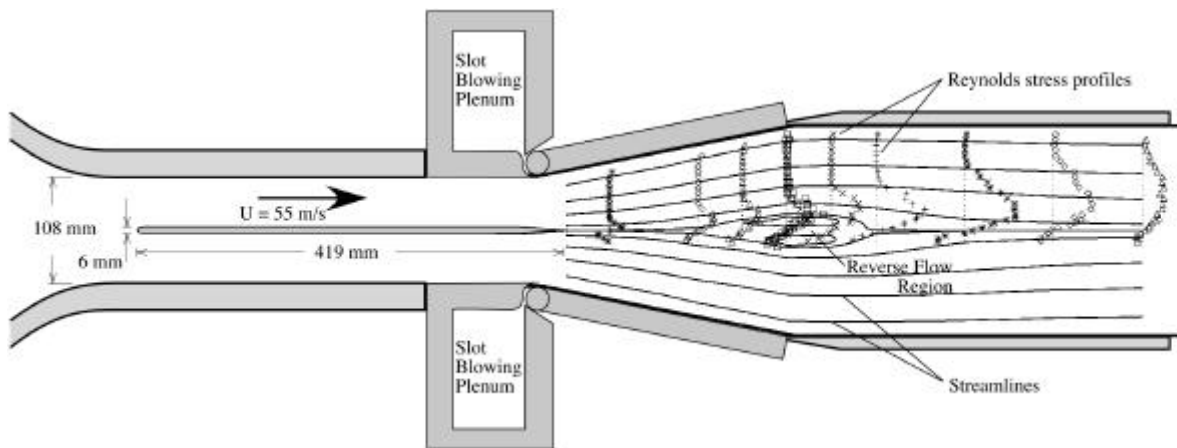
Figure 9. Wake in adverse pressure gradient experimental setup and results. Results shown as streamlines with Reynolds shear stress plotted at several axial locations. Adverse pressure gradient is sufficient in this configuration to cause wake flow to reverse direction.[23]

Figure 10. Three-element wing with part-span high-lift system in 7- by 10-Foot Wind Tunnel.
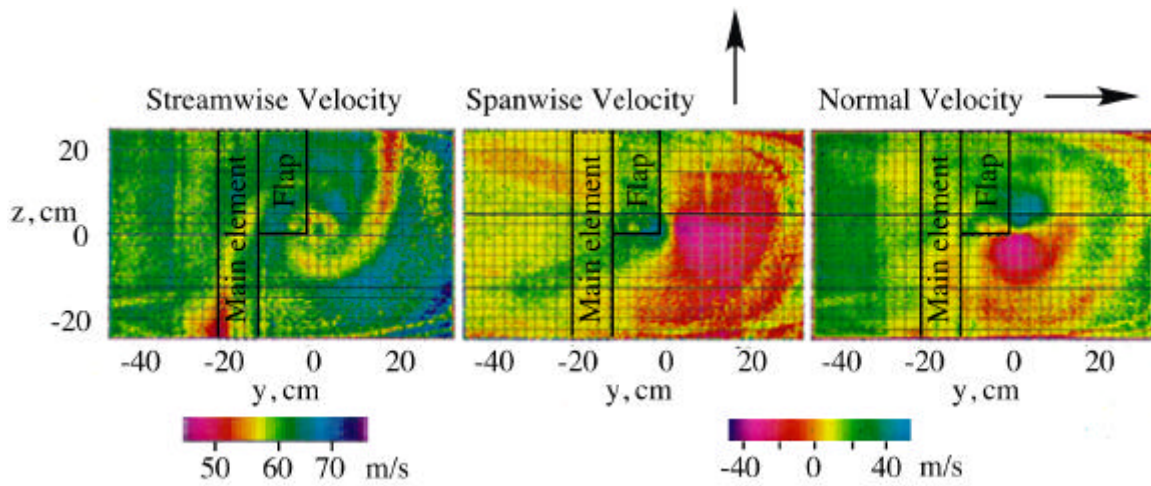
Figure 11. PDV measurements of flap-tip vortex in 7- by 10-Foot Wind Tunnel; M = 0.2, 35° flap deflection, 10° angle of attack, slat removed.[26]

16
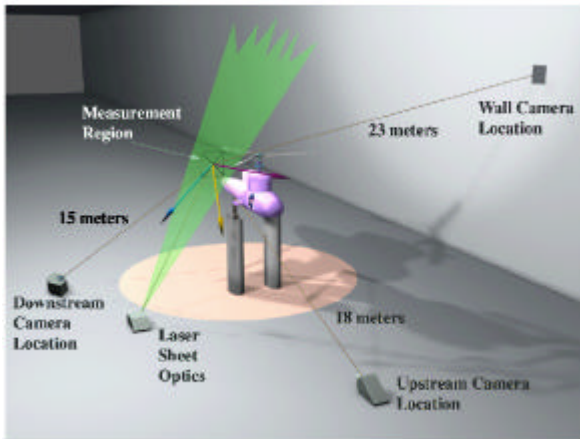
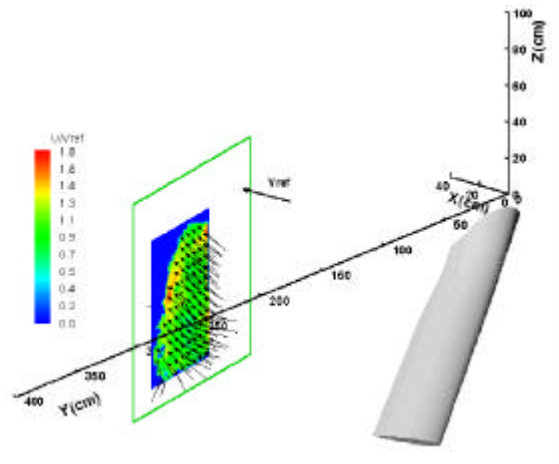Figure 12. Experimental setup of PDV in 80- by 120-Foot Wind Tunnel for rotor wake measurements.

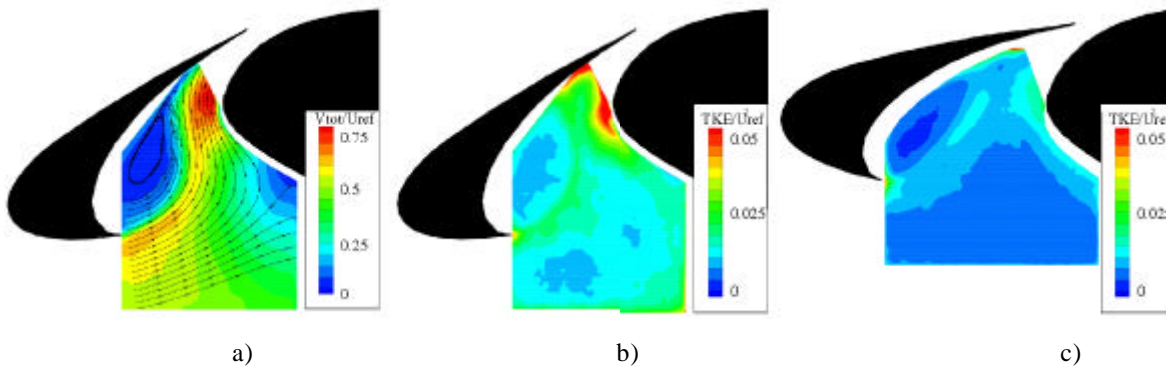Figure 13. PDV velocity measurements of rotor wake with blade 30° past measurement plane. Color contours represent velocity normal to plane.[27]

a)   b)   c)

Figure 14. In-plane velocity measurements of the flow on lee side of leading-edge slat in 7- by 10-Foot Wind Tunnel (M = 0.1, 25° nose-down slat deflection, 35°flap deflection; a) mean velocity, b) unsteady kinetic energy, c) unsteady kinetic energy for slat deployed 5° nose down.[9]
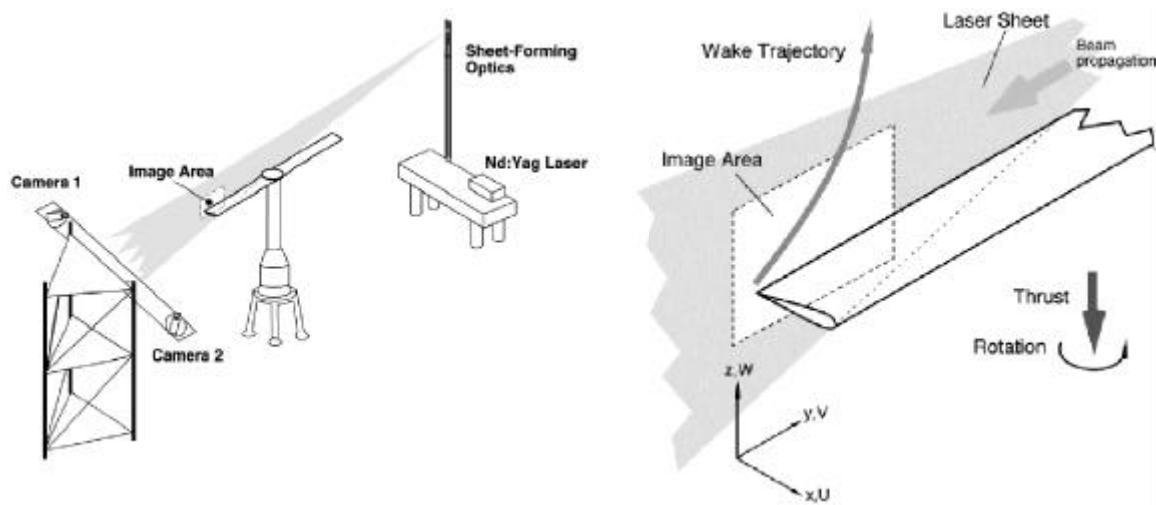
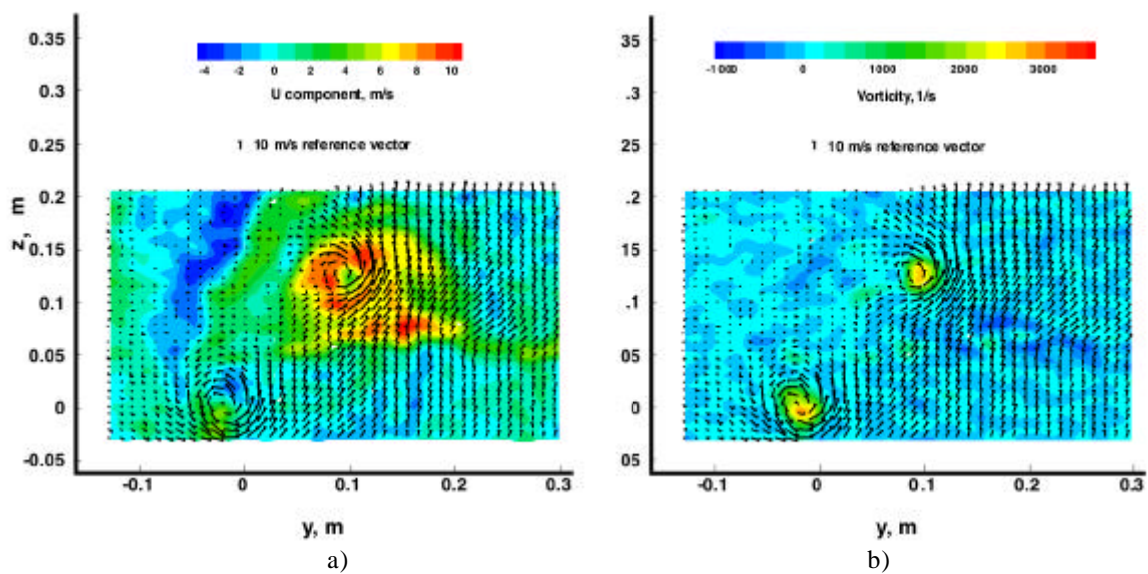Figure 15. 3DPIV set up for measuring rotor wake in hover.

a)

b)

Figure 16. Instantaneous velocity vectors in the measurement plane. Color contours show: a) normal velocity, b) out of plane vorticity.[32]
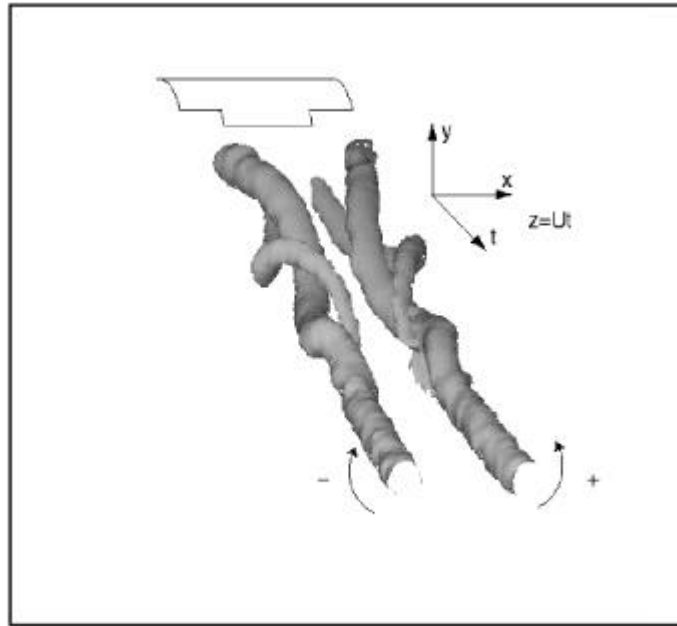
Figure 17. PIV measurements of wake vortex development behind simplified wing with a flap. Iso-surface of vorticity. Data corresponds to a distance from 0 to 100 spans aft of the wing. Merging of the co-rotating tip/flap vortex pairs after one orbit is clearly evident.[38]